

Guided Decoding for Robot On-line Motion Generation and Adaption

Nutan Chen^{1*}, Botond Cseke^{1*}, Elie Aljalbout^{1,2},
 Alexandros Paraschos¹, Marvin Alles¹, Patrick van der Smagt^{1,3}

Abstract— We present a novel motion generation approach for robot arms, with high degrees of freedom, in complex settings that can adapt online to obstacles or new via points. Learning from Demonstration facilitates rapid adaptation to new tasks and optimizes the utilization of accumulated expertise by allowing robots to learn and generalize from demonstrated trajectories. We train a transformer architecture, based on conditional variational autoencoder, on a large dataset of simulated trajectories used as demonstrations. Our architecture learns essential motion generation skills from these demonstrations and is able to adapt them to meet auxiliary tasks. Additionally, our approach implements auto-regressive motion generation to enable real-time adaptations, as, for example, introducing or changing via-points, and velocity and acceleration constraints. Using beam search, we present a method for further adaption of our motion generator to avoid obstacles. We show that our model successfully generates motion from different initial and target points and that is capable of generating trajectories that navigate complex tasks across different robotic platforms.

I. INTRODUCTION

Motion generation is a challenging topic for robot arms with high degrees of freedom (DoF). One main challenge is to generate smooth trajectories to solve a given task while ensuring the robot and its environment's safety, and respecting the robot's embodiment constraints. This problem is especially complex when the task involves auxiliary objectives beyond reaching a target point, such as avoiding obstacles, passing via specified points, or imposing velocity or acceleration constraints. Another particularly intriguing aspect of motion generation is the incorporation of learning from demonstration (LfD) within the same process. Allowing users or agents to present a guiding trajectory based on prior knowledge helps the rapid development of robotic applications. This capability is crucial for adapting to novel tasks and leveraging accumulated expertise effectively. Motion primitives offer a promising avenue for achieving this goal [1], [2], [3], [4]. By encapsulating fundamental motion behaviors into primitives, the robot can learn and generalize from demonstrations, promoting versatility and adaptability in complex tasks. Integrating learning from demonstration with the challenges of motion generation presents an exciting direction for advancing the capabilities of robot arms with high degrees of freedom.

¹During this work, all Authors were affiliated with the Machine Learning Research Lab, Volkswagen Group, Germany <first-name>.<last-name>@volkswagen.de

²Elie Aljalbout is currently with the Robotics and Perception Group, at the Department of Informatics of the University of Zurich (UZH) and the Department of Neuroinformatics at UZH and ETH Zurich, Switzerland.

³Faculty of Informatics, Eötvös Loránd University, Budapest, Hungary

* These authors contributed equally to this work.

Traditional approaches to motion primitives often rely on a limited number of demonstrations, focusing primarily on adapting learned motions [2], [3]. However, these methods struggle with generalization when applied to new or variations of the learned tasks that go beyond simple interpolation. Our work seeks to address these limitations by leveraging generative models, specifically an autoregressive framework, which allows learning from extensive datasets and significantly improves generalization. Unlike diffusion-based models, our autoregressive model facilitates online motion adaptation. Diffusion-based models [5] require multiple iterations to generate a full trajectory and, therefore, can not adapt fast to changes in the environment or the robot embodiment. In contrast our autoregressive model supports the integration of online feedback, allowing it to adapt to changes to the task, e.g. different via-points, obstacle locations, or the robot, e.g. acceleration constraints arises from interacting with physical objects.

In this work, we propose a framework for learning motion generation. We create a large dataset of robot motion trajectories with multiple simulated robots and train a transformer architecture to learn to generate motion based on given initial and target points. We design a Transformer conditional variational autoencoder. The trained generative model encapsulates basic motion generation skills based on the training data. We further propose an approach to efficiently adapt the generated motion to satisfy auxiliary tasks and constraints such as obstacle avoidance, via points and velocity constraints. The process is auto-regressive allowing for integrating feedback from the real system during motion generation. Our approach allows for generating motion based on an initial and target point only, or to imitate a full trajectory given by a user or external agent. Our experiments show the usability of our method for imitating and adapting user-given trajectories to a given task, such as via point constraints, obstacles, and velocity and acceleration constraints. We also show the benefits of training with data collected using various robots.

II. METHODS

We design a model to encode and generate robot trajectories by leveraging a transformer-based architecture. We generate trajectories in an autoregressive manner, allowing for real-time adaptation to constraints such as obstacle avoidance and velocity limits. In this section, we present a Transformer-based autoencoder model with an autoregressive decoder and the online adaptation methods that are tailored to this decoder.

A. Inference model for the infilling task

We consider a dataset $\mathcal{D} = \{x^{(i)}\}_{i=1}^N$ of trajectories $x^{(i)} = \{x_t^{(i)}\}_{t=1}^T$ and our goal is to learn representations that can help us generate new trajectories given a starting point x_1 and an endpoint x_T . We propose to do this with the Conditional VAE [6] model

$$p_\theta(x_{2:T-1}|x_{1,T}) = \int p_\theta(x_{2:T-1}|x_{1,T}, z) p_\theta(z|x_{1,T}) dz,$$

where the latent variables (representations) z are expected to encode features of paths with starting point x_1 and endpoint x_T . Since the likelihood is analytically intractable, we learn this model by approximate maximum likelihood via a variational bound. We minimize the negative evidence lower bound (ELBO)

$$L(\theta, \phi) = -\mathbb{E}_{\hat{p}(x_{1:T})} \mathbb{E}_{q_\phi(z|x_{1:T})} [\log p_\theta(x_{2:T-1}|x_{1,T}, z)] + \mathbb{E}_{\hat{p}(x_{1:T})} \text{KL}[q_\phi(z|x_{1:T}) \| p_\theta(z|x_{1,T})].$$

Here $p_\theta(z|x_{1,T})$ is the conditional prior model, $p_\theta(x_{2:T-2}|x_{1,T}, z)$ is the decoder/generation model, and $q_\phi(z|x_{1:T})$ is the encoder/recognition or (variational) approximate posterior distribution model. The training method can be found in App. A. To generate a new trajectory, we sample a latent feature z from the learnt prior $z \sim p_\theta(z|x_{1,T})$. We then use the feature z as a conditioning variable in the learnt decoder model $p_\theta(x'_{2:T-2}|x_{1,T}, z)$.

In this paper we use an autoregressive decoder model $p_\theta(x'_{2:T-2}|x_{1,T}, z) = \prod_t p_\theta(x'_{t+1}|x'_{2:t}, x_{1,T}, z)$. We do this because it is a more natural choice for doing online trajectory guidance and adaptation compared to methods that generate a whole trajectory like, for example, diffusion probabilistic models [7].

Either the prior or the autoregressive decoder is capable of generating diverse samples. To enhance adaptability and generalization, our model incorporates both for distinct purposes. With a fixed demonstration/posterior, we can adjust the trajectories from the decoder. Conversely, by specifying a starting and ending point, we can generate various trajectories using the prior.

B. PerceiverIO encoder

We define an encoder $q_\phi(z|x_{1:T})$ that is architecturally similar to a PerceiverIO model [8], that is, a multi-layered, attention-based neural architecture where the initial block uses cross-attention (CA) layer and the subsequent blocks use a shared self-attention (SA) layer

$$\begin{aligned} h_{1:K}^{(1)} &= \text{RMLP}_\phi \circ \text{RCA}_\phi(h_{1:K}^{(0)}, \tilde{x}_{1:T}) \\ h_{1:K}^{(l+1)} &= \text{RMLP}_\phi \circ \text{RSA}_\phi(h_{1:K}^{(l)}), \quad l = 1, \dots, L \end{aligned}$$

The initial layer $h_{1:K}^{(0)}$ is a learned parameter, a part of ϕ . The values $\tilde{x}_t = Wx_t + \tau_t$ are embedding the data into the hidden space via a linear layer W and a positional embedding τ_t . RCA and RSA denote a residual (R) cross-attention and a residual self-attention block defined as $\text{RCA}(h, z) = \text{LayerNorm}(h + \text{CA}(h, z))$ and $\text{RSA}(h) = \text{LayerNorm}(h + \text{SA}(h))$, respectively. RMLP denotes a

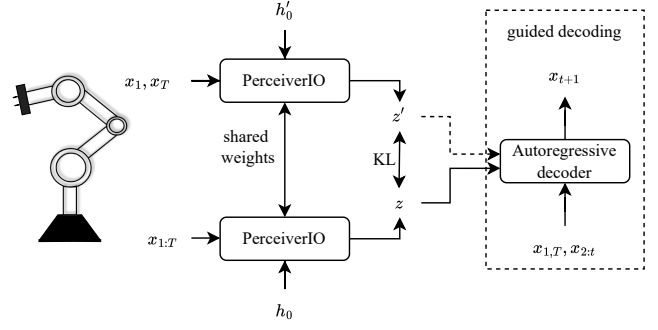


Fig. 1: Model overview. Each PerceiverIO module gets a trajectory, but for the prior it only contains the beginning and end points and a full trajectory for the posterior. During training, minimizing the KL divergence between the two makes the representation of the PerceiverIO module that only gets x_1 and x_T generates the same latent distribution as the one getting the full trajectory; therefore, it learns interpolation. The latent state then is used by the autoregressive decoder to generate the next setpoint x_{t+1} . Dashed lines indicate components used exclusively during the post-training adaptation phase, not included in the initial training process.

residual MLP block with one hidden layer. Note that the resulting self-attention block is a shared block. The encoder is then defined as a diagonal multivariate Gaussian distribution $q_\phi(z|x_{1:T}) = \mathcal{N}(z; \mu_\phi^{\text{enc}}(h^{(L)}), \sigma_\phi^{\text{enc}}(h^{(L)})^2)$ with μ_ϕ^{enc} and σ_ϕ^{enc} being simple MLPs. The latent variable z is thus designed to encode the trajectory $x_{1:T}, x_t \in \mathbb{R}^d$ to a shorter sequence of K variables $z = \{z_k\}_{k=1}^K, z_k \in \mathbb{R}^m$ (K is a chosen hyper-parameter). Note that the choice $K = 1$ results in a single vector embedding of the trajectory $x_{1:T}$.

To implement the prior $p_\theta(z|x_{1,T})$ we use the same model having as input only the pair $\{x_1, x_T\}$.

This type of Perceiver architecture is designed to reduce the quadratic $(T \times T)$ computational complexity of a Transformer encoder model (self-attention layers) on $x_{1:T}$ by cross-attending the sequence $(T \times K)$ and performing less computationally demanding self-attentions $(K \times K)$ on $z_{1:K}$. Generally, there is a large class of Perceiver models/blocks with learnable queries or latents that are used for transforming data between different modalities/embedding sizes, for example, a Perceiver model with K queries can be used as a head-block in a classification model with K classes.

C. Autoregressive decoder

A natural choice for the decoder in the context of attention-based models is a conditional autoregressive model

$$p_\theta(x_{2:T-1}|x_{1,T}, z) = \prod_{t=1}^{T-1} p_\theta(x_{t+1}|x_{2:t}, x_{1,T}, z).$$

Here, we again use an attention-based neural architecture, a standard transformer decoder [9] defined as

$$h_{1:T}^{(l+1)} = \text{RMLP}_\theta^{(l+1)} \circ \text{RCA}_\theta^{(l+1)}(\cdot, z) \circ \text{RCSA}_\theta^{(l+1)}(h_{1:T}^{(l)})$$

with $h_{1:T}^{(0)} = \tilde{x}_{1:T}$ being the embeddings as defined in the previous section. The data $x_{1:T}$ together with the representation z are direct inputs to the decoder with which the trajectory generation starts. To allow for flexible output length, we do not fix the position of x_T at the end; instead, we set it as the first step of the input. The value $h_t^{(L)}$ is then used to define the autoregressive model $p(x_{t+1}|x_{2:t}, x_{1:T}, z) = \mathcal{N}(x_{t+1}; \mu_\theta^{\text{dec}}(h_t^{(L)}), \sigma_\theta^{\text{dec}}(h_t^{(L)})^2)$. The additional ‘‘C’’ in the layer definition in RCSA denotes a causal attention model implemented via triangular attention masks. Unlike in Transformers models for text infilling [10], [11], we do not need to include segmentation embedding since the length and position of the start and end points in the model are already provided.

D. Training-free trajectory generator—adaptive decoding

In addition to learning a conditional autoencoder model for trajectory generation, we would also like to extend the model to be able to perform online trajectory adaptation, for example, to add via-points and obstacle avoidance. To achieve this, we do online (approximate) probabilistic inference using $p_\theta(x_{t+1}|x_{1:t}, x_T, z)$ without updating the model parameter θ . The obvious choice is a Bayesian approach where the adaptation can be formulated as a Bayesian update of $p_\theta(x_{t+1}|x_{1:t}, x_T, z)$, via a likelihood $p(y_{t+1}|x_{t+1})$. Alternatively, the likelihood can also be used to implement constraints, for example, a Bayesian update with a likelihood function $I_{[a,b]}(x)$ can implement trajectory boundaries $a_i \leq x_i \leq b$.

To use generic constraints, we can formulate online trajectory adaptation as the constrained optimisation problem

$$\min_{q(x_{t+1})} \text{KL}[q(x_{t+1}) \| p_\theta(x_{t+1}|x_{1:t}, x_T, z)] \quad (1)$$

$$\text{s.t. } \mathbb{E}_{q(x_{t+1})}[H(c(x_{t+1}))] \leq \alpha, \quad (2)$$

where $H(\cdot)$ is the Heaviside function and $c(\cdot)$ is a desired constraint function. The constraint in (2) expresses what proportion $0 \leq \alpha \leq 1$ of the probability mass is allowed not to satisfy the constraint, see for example [12]. The KL objective is convex in q , the constraints are linear, and the optimal solution (q^*, λ^*) satisfies

$$q^*(x_{t+1}) \propto p_\theta(x_{t+1}|x_{1:t}, x_T, z) \times \exp\{-\lambda^* H(c(x_{t+1}))\}.$$

Solving this optimization, however, even for a Gaussian q and a constraint c implementing simple boundary constraints can be numerically demanding. For more general constraints such as obstacle avoidance, (2) can be analytically intractable. For this reason, in the following we will only exploit the form of $q^*(x_{t+1})$ to propose fast online trajectory adaptation methods. Various trajectory adaptations can be conveniently formulated either as (1) by choosing the appropriate constraint function $c(\cdot)$ or as a Bayesian update with the appropriate likelihood. These will be detailed in the following.

E. Implementing specific constraints

1) *Obstacle avoidance with beam search:* Beam search (BS) [13] is a classic heuristic in the field of natural language

processing (autoregressive models). It is used to generate trajectories with high likelihood or other specific score values. The method recursively generates trajectories as follows. A set of S trajectories $\{x_{2:t}^{(s)}\}$ are stored together with their scores, for example, the path likelihood $\log p(x_{2:t}^{(s)}|x_{1:T}, z)$. For each trajectory S new samples $x_{t+1}^{(s,r)} \sim p(x_{t+1}|x_{2:t}^{(s)}, x_{1:T}, z)$, $r = 1, \dots, S$ are generated as candidates and the corresponding total scores are computed for the extended trajectories $(x_{2:t}^{(s)}, x_{t+1}^{(s,r)})$ for all pairs (s, r) . The overall top S extended trajectories are selected for the next step. Inspired by the form of $q^*(x_{t+1})$, we define the score by adding $\tilde{s}(x_{t+1}) = -\gamma \max(c(x_{t+1}), 0)$ with $c(x) = \delta^2 - \|x - x_{\text{obstacle}}\|^2$ to the likelihood.

2) *Position, velocity and acceleration bounds:* Simple position and velocity bounds in an interval $[a, b]$ can be implemented via a Bayesian update. In case of position bounds the posterior, $q(x_{t+1}) \propto I_{[a,b]}(x_{t+1}) p_\theta(x_{t+1}|x_{1:t}, x_T, z)$ is a truncated Gaussian from which we can easily sample. In case of velocity bounds $[v_{\min}, v_{\max}]$, we notice that $v_t = (x_{t+1} - x_t)/\Delta t$ is Gaussian to which we can apply a Bayesian update via $I_{[v_{\min}, v_{\max}]}(v_t)$. Due to the fact that the predictive distribution is a diagonal (independent) Gaussian, this results in a truncated Gaussian distribution on v_{t+1} and subsequently on x_{t+1} . Acceleration bounds follow the same principle applied to $a_t = (x_{t+1} - 2x_t + x_{t-1})/\Delta t^2$.

3) *Via points through Brownian bridge:* To add additional via-points to the autoregressive model $p_\theta(x_{t+1}|x_{1:t}, x_T, z)$, say, x_s at an intermediate time $1 < s < T$ we would have to compute the Bayesian posterior

$$\begin{aligned} p(x_{t+1}|x_{1:t}, x_s, x_T, z) \\ \propto p(x_s|x_{t+1}, x_{1:t}, x_T, z) \times p(x_{t+1}|x_{1:t}, x_T, z). \end{aligned}$$

Since the likelihood term $p(x_s|x_{t+1}, x_{1:t}, x_T, z)$ is intractable, we propose to approximate it with a Gaussian likelihood

$$p(x_s|x_{t+1}, x_{1:t}, x_T, z) \approx \mathcal{N}(x_s|x_{t+1}, (s-t-1) \sigma_{\text{vp}}^2).$$

To have a stronger conditioning on the past $x_{1:t}$ we can alternatively use a Brownian-bridge approximation

$$\mathcal{N}\left(x_{t+1}|x_t + \frac{1}{s-t}(x_s - x_t), \sigma_{\text{vp}}^2 \frac{s-t-1}{s-t}\right).$$

Both of the above approximations lead to a Gaussian approximation of $p(x_{t+1}|x_{1:t}, x_s, x_T, z)$.

4) *Constrained Beam Search for Brownian bridge (optional):* Drawing on the Constrained Beam Search (CBS) described by [14], we refine the approach by integrating a controller. This addition drives the generated trajectory towards the desired outcome, rather than substituting words.

We generate samples of x_{t+1} for each sample x_t , using the Transformer decoder incorporating via point method, i.e., Brownian Bridge. We categorize the generated trajectories into three banks: Bank-0 for trajectories that do not meet the constraint; Bank-1 for trajectories that have applied the controller but still do not satisfy the constraint; and Bank-2 for trajectories that satisfy the constraint. For the trajectory $x_{1:t}$ that satisfies the via-point constraint, we generate a single

sample of x_{t+1} using the Transformer decoder exclusively for Bank-2. If $x_{1:t}$ fails to satisfy the constraint, we then generate one x_{t+1} sample from the Transformer decoder with the controller. In this case, if x_{t+1} satisfies the constraint, the sample is allocated to Bank-2; otherwise, it goes to Bank-1. Lastly, in cases where $x_{1:t}$ does not satisfy the constraint, we generate N_s x_{t+1} samples from the Transformer decoder only. Here, if x_{t+1} satisfies, the sample is classified into Bank-2; if not, into Bank-0. Following this, we select the samples iteratively from each bank with the order of Bank-2, Bank-1, Bank-0, based on the negative log-likelihood criterion until we have N_s samples in total for x_{t+1} .

Previous work [14] has demonstrated that CBS outperforms BS during guided language generation, akin to via point task in robot trajectory generation. However, for tasks such as obstacle avoidance, only BS is applicable, since Bank0 and Bank1 cannot be defined.

III. RELATED WORK

In robotics, movement primitives are used to specify behavior based on human-demonstrated trajectories. Dynamic movement primitives (DMP) take inspiration from dynamical systems to specify motion behavior [1], [2]. DMPs use human demonstrations to fit a forcing term that augments the attractor dynamics to match the demonstrated trajectories. DMPs allow motion adaptation, such as avoidance of obstacles, by adding additional terms such as repulsive fields to their driving equation [15], [16]. This process should be done carefully to avoid competing objectives. Furthermore, DMPs applied in latent space [17], [18] provide the capability to adjust motions within this latent space. Unlike these works which adapt the latent space incrementally, our approach is a sequence-to-sequence model. In our model, each trajectory is mapped to a distinct point in the latent space, affording greater flexibility in guiding the decoder's output. Probabilistic movement primitives represent trajectory distributions, which simplifies the blending of multiple trajectories [3]. Adapting movement to auxiliary tasks is also possible within this framework [12], [19], [20]. Riemannian motion policies easily allow the combination of multiple behaviors in both the task and the configuration space [4]. However, this method lacks the advantages of probabilistic formulations.

Recently, diffusion models [7] for motion generation [5] have been developed. However, these models generally require a large number of iterations to transform Gaussian noise into usable data, which is computationally intensive. In addition, it can only produce complete sequence data. In contrast, our model does not require multiple iterations for completion and is an autoregressive model that generates data for each time step which is more useful for online motion adaption.

IV. EXPERIMENTS

A. Data Collection

To train our models we collect a large dataset of robot motion trajectories in simulation. We use the NVIDIA

IsaacSim simulator to generate a large amount of data in parallel. Our main experiments are based on data using the Franka Emika Panda robot. However, for the multi-robot experiment we also introduce motion data from different robots, namely Rethink Robotic's Sawyer, Kuka's LBR IIWA 7, Jaco and Kinova Gen3 from Kinova Robotics, and Universal Robot's UR5e. We generate samples for each robot in 4096 environments in parallel and repeat this process for multiple episodes. At the beginning of each episode, we randomly sample starting and end-goal positions in the configuration space. We then use a proportional derivative controller to drive the robot to the goal position. To generate more diverse trajectories, we occasionally sample via points at the beginning of an episode and use these as target points for a short while at the beginning of the episode.

For the trajectory of the end-effector, we have $x \in \mathbb{R}^3$, while $x \in \mathbb{R}^7$ for joint space. The robots which have 6-DOF are padded zero to match this representation. Each sequence has a total length of $T = 64$.

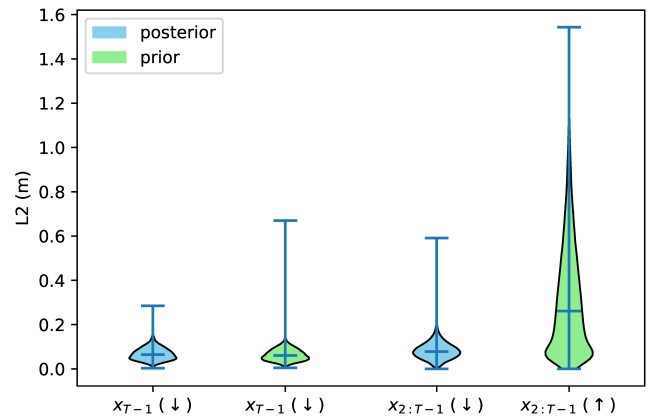


Fig. 2: Distances to the original trajectories for the Panda robot in Cartesian space.

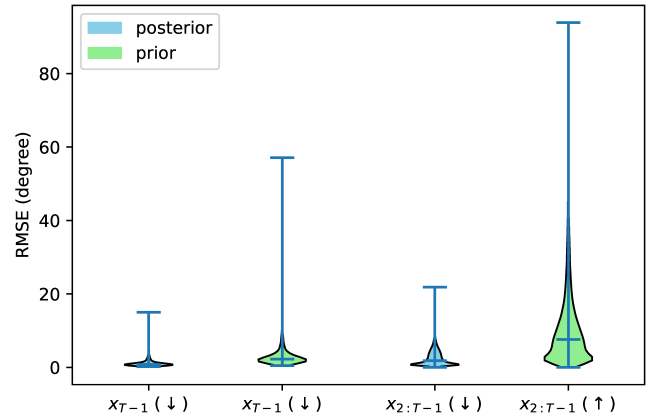


Fig. 3: Distances to the original trajectories for IIWA robot in joint space.

TABLE I: Velocity and acceleration limits.

methods	samples	max values
velocity bound	prior	0.050
	posterior	0.050
	boundary	0.050
	original data	0.094
acceleration bound	prior	0.020
	posterior	0.020
	boundary	0.020
	original data	0.031

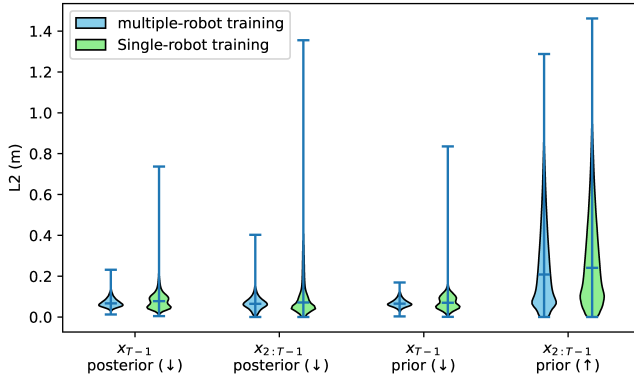


Fig. 4: Distances to the original trajectories for the Panda robot in Cartesian space with multiple-robot training and single-robot training.

B. Distances to the original trajectories

We split the dataset into 20,000 training, 2048 validation, and 2048 test samples. A single robot was trained and then evaluated on its performance. Fig. 2 and 3 illustrate the generalization from the prior and the reconstruction. Evaluation metrics include the Root Mean Square Error (RMSE) measured in degrees for joint movements, and an L2 Norm, measured in meters, for assessing the trajectories for the end-effector. Assuming endpoint distances are the same, a larger distance for trajectories from the prior distribution to the original demos is advantageous, as it demonstrates the *diversity* of the learned prior. Except that, lower distance values to the original samples indicate better performance, where the distance reflects the *fidelity* of the model's output approximating the original trajectories. Rather than determining the endpoint distance, we calculate the distance at x_{T-1} , since the x_T is given.

C. Generalization on an unknown robot

Scaling up models across various robots presents significant challenges but offers substantial benefits, as noted in [21]. To assess our model's ability to generalize, we conducted an experiment involving different robots. In this experiment, the training dataset comprises IWA, UR5e, and Sawyer robots operating in Cartesian space. The validation dataset uses the Jaco robot, while the Panda robot is the test dataset. For

comparison of single-robot training, the training dataset was divided into three subsets, each corresponding to a specific robot, with the same validation and test datasets used across all experiments. The results from the single-robot training are aggregated for presentation. As illustrated in Fig. 4, training across multiple robots demonstrates superior generalization to an unknown robot.

D. Adaptation and generalization

The experiments are trained on a Panda robot. Our adaption and generalization are suitable for both samples from priors and posterior. To enhance visualization and compare with demonstrations, we present all results based on samples from posteriors, except for those in Sections IV-D.4 and IV-D.2 which also use samples from priors.

1) *Position bound*: As depicted in Figure 5, the generated trajectories are supposed to follow the original demonstrations, with adaptations made to ensure compatibility within the cuboid boundaries.

2) *Velocity and acceleration bound*: We have established boundaries for both velocity and acceleration, as detailed in Table I. Although the table presents only a single boundary for each type of boundary, these boundaries can be set to arbitrary values.

3) *Via points*: We adapted the movements for via point (see Fig. 6) using the Brownian bridge. We set the hyperparameter σ_{vp} in a similar range of the output σ from the autoregressive decoder. The experiments show the comparisons between via points without and with CBS, where the beam search size is set to five. The findings indicate that when CBS is used, the trajectories appear more natural and closer to the original demos. On the contrary, as CBS is a historical search method, a Brownian bridge without CBS enables online trajectory generation.

4) *Obstacle avoidance*: In the experiment, we used a beam search with a size of 25. The temperature of the output, which is the scale of the output STD, was set to two. Fig. 7 demonstrates how the adapted trajectories effectively navigate to avoid spherical obstacles for samples drawn from both the prior and posterior distributions.

V. CONCLUSION

In this paper we introduce a novel Transformer-based auto-encoder framework for robot motion generation and adaptation, leveraging Learning from Demonstration (LfD). The latent space of the autoencoder can be viewed a motion representation similarly as in movement primitives. The conditioning of the trajectory generation on goal an motion representation is implemented through flexible cross-attention mechanisms. By using an autoregressive decoder and online (approximate) inference methods our approach generates trajectories that adapt to various task space constrains such as obstacle avoidance, via-points, and various position, velocity, and acceleration bounds. The experiments validated the framework's robustness and adaptability across different robots and various trajectory constraints.

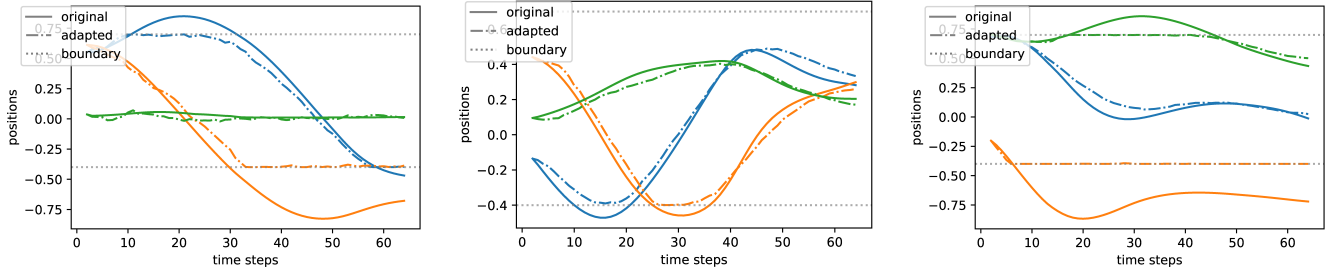


Fig. 5: Motion adaptation for position boundary. Colors indicate the axes of the Cartesian coordinate.

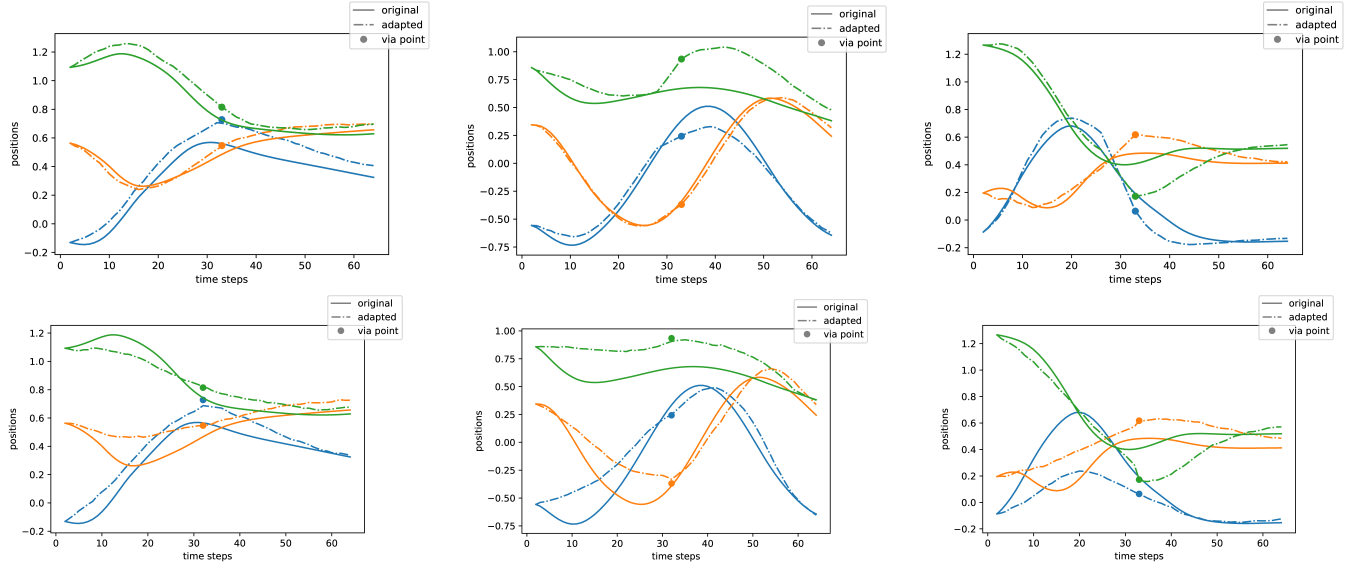


Fig. 6: Brownian bridge for via point with (upper) and without (lower) CBS. Colors indicate the axes of the Cartesian coordinate.

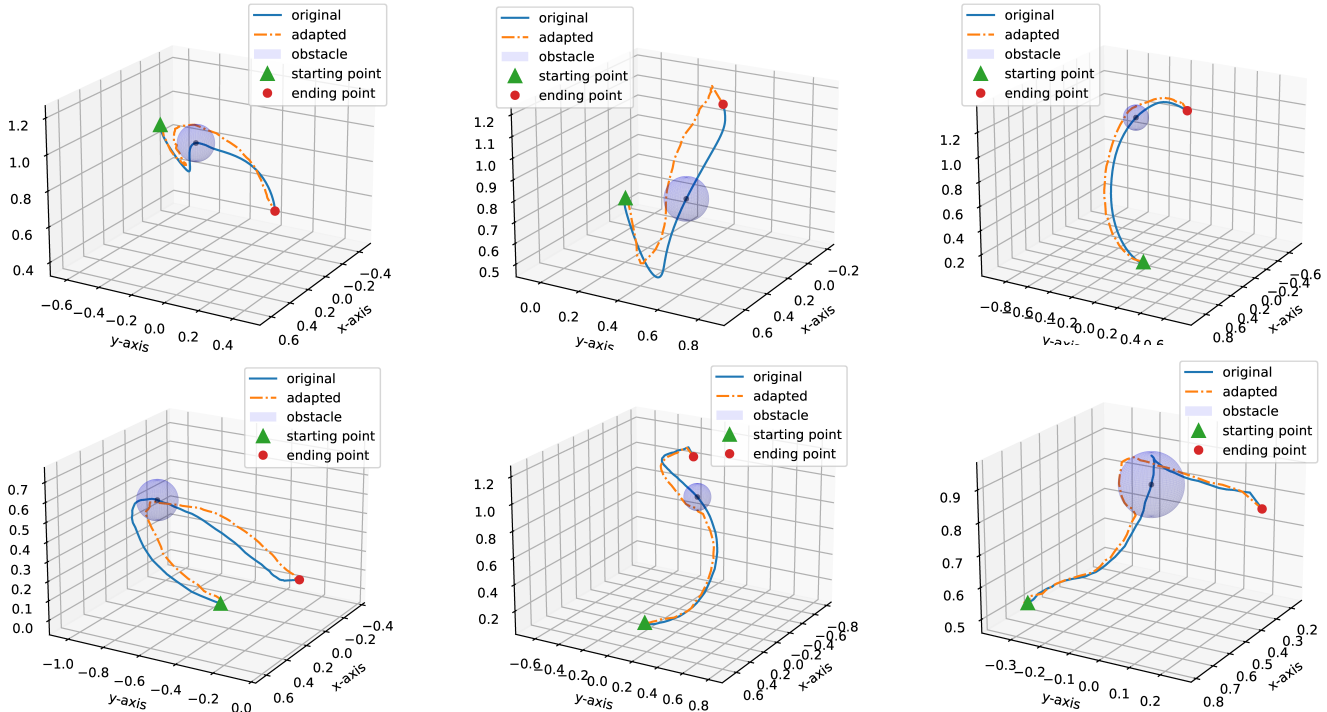


Fig. 7: Adaption for obstacle avoidance. (Upper) Obstacle avoidance with the samples from the posterior. (Lower) Obstacle avoidance with samples from the prior, where the original refers to the samples from the prior without adaptation of the decoder. All of them successfully avoid the obstacles, although the visualization is not perfect due to the viewpoint.

REFERENCES

[1] S. Schaal, “Dynamic movement primitives-a framework for motor control in humans and humanoid robotics,” in *Adaptive motion of animals and machines*. Springer, 2006, pp. 261–280.

[2] A. J. Ijspeert, J. Nakanishi, H. Hoffmann, P. Pastor, and S. Schaal, “Dynamical movement primitives: learning attractor models for motor behaviors,” *Neural computation*, vol. 25, no. 2, pp. 328–373, 2013.

[3] A. Paraschos, C. Daniel, J. R. Peters, and G. Neumann, “Probabilistic movement primitives,” *Advances in neural information processing systems*, vol. 26, 2013.

[4] N. D. Ratliff, J. Issac, D. Kappler, S. Birchfield, and D. Fox, “Riemannian motion policies,” *arXiv preprint arXiv:1801.02854*, 2018.

[5] M. Janner, Y. Du, J. B. Tenenbaum, and S. Levine, “Planning with diffusion for flexible behavior synthesis,” *arXiv preprint arXiv:2205.09991*, 2022.

[6] K. Sohn, H. Lee, and X. Yan, “Learning structured output representation using deep conditional generative models,” *NIPS*, vol. 28, 2015.

[7] J. Ho, A. Jain, and P. Abbeel, “Denoising diffusion probabilistic models,” *Advances in neural information processing systems*, vol. 33, pp. 6840–6851, 2020.

[8] A. Jaegle, F. Gimeno, A. Brock, O. Vinyals, A. Zisserman, and J. Carreira, “Perceiver: General perception with iterative attention,” in *International conference on machine learning*. PMLR, 2021, pp. 4651–4664.

[9] A. Vaswani, N. Shazeer, N. Parmar, J. Uszkoreit, L. Jones, A. N. Gomez, Ł. Kaiser, and I. Polosukhin, “Attention is all you need,” *Advances in neural information processing systems*, vol. 30, 2017.

[10] J. Devlin, M.-W. Chang, K. Lee, and K. Toutanova, “Bert: Pre-training of deep bidirectional transformers for language understanding,” *arXiv preprint arXiv:1810.04805*, 2018.

[11] T. Wang and X. Wan, “T-cvae: Transformer-based conditioned variational autoencoder for story completion.” in *IJCAI*, 2019, pp. 5233–5239.

[12] F. Frank, A. Paraschos, P. van der Smagt, and B. Cseke, “Constrained probabilistic movement primitives for robot trajectory adaptation,” *IEEE Transactions on Robotics*, vol. 38, no. 4, pp. 2276–2294, 2021.

[13] P. Koehn, *Statistical machine translation*. Cambridge University Press, 2009.

[14] M. Post and D. Vilar, “Fast lexically constrained decoding with dynamic beam allocation for neural machine translation,” *arXiv preprint arXiv:1804.06609*, 2018.

[15] D.-H. Park, H. Hoffmann, P. Pastor, and S. Schaal, “Movement reproduction and obstacle avoidance with dynamic movement primitives and potential fields,” in *Humanoids 2008-8th IEEE-RAS International Conference on Humanoid Robots*. IEEE, 2008, pp. 91–98.

[16] H. Hoffmann, P. Pastor, D.-H. Park, and S. Schaal, “Biologically-inspired dynamical systems for movement generation: Automatic real-time goal adaptation and obstacle avoidance,” in *2009 IEEE International Conference on Robotics and Automation*, 2009, pp. 2587–2592.

[17] N. Chen, J. Bayer, S. Urban, and P. Van Der Smagt, “Efficient movement representation by embedding dynamic movement primitives in deep autoencoders,” in *2015 IEEE-RAS 15th international conference on humanoid robots (Humanoids)*. IEEE, 2015, pp. 434–440.

[18] N. Chen, M. Karl, and P. Van Der Smagt, “Dynamic movement primitives in latent space of time-dependent variational autoencoders,” in *2016 IEEE-RAS 16th international conference on humanoid robots (Humanoids)*. IEEE, 2016, pp. 629–636.

[19] D. Koert, G. Maeda, R. Lioutikov, G. Neumann, and J. Peters, “Demonstration based trajectory optimization for generalizable robot motions,” in *2016 IEEE-RAS 16th International Conference on Humanoid Robots (Humanoids)*, 2016, pp. 515–522.

[20] D. Koert, J. Pajarin, A. Schotschneider, S. Trick, C. Rothkopf, and J. Peters, “Learning intention aware online adaptation of movement primitives,” *IEEE Robotics and Automation Letters*, vol. 4, no. 4, pp. 3719–3726, 2019.

[21] A. Padalkar, A. Pooley, A. Jain, A. Bewley, A. Herzog, A. Irpan, A. Khazatsky, A. Rai, A. Singh, A. Brohan, *et al.*, “Open x-embodiment: Robotic learning datasets and rt-x models,” *arXiv preprint arXiv:2310.08864*, 2023.

[22] T. Sønderby, C. K. and Raiko, L. Maaløe, S. K. Sønderby, and O. Winther, “Ladder variational autoencoders,” *NeurIPS*, 2016.

[23] S. R. Bowman, L. Vilnis, O. Vinyals, A. M. Dai, R. Jozefowicz, and S. Bengio, “Generating sentences from a continuous space,” *arXiv preprint arXiv:1511.06349*, 2015.

[24] D. P. Kingma, T. Salimans, R. Jozefowicz, X. Chen, I. Sutskever, and M. Welling, “Improved variational inference with inverse autoregressive flow,” *Advances in neural information processing systems*, vol. 29, 2016.

[25] A. Roberts, J. Engel, C. Raffel, C. Hawthorne, and D. Eck, “A hierarchical latent vector model for learning long-term structure in music,” in *International conference on machine learning*. PMLR, 2018, pp. 4364–4373.

[26] D. J. Rezende and F. Viola, “Taming VAEs,” *CoRR*, 2018.

[27] A. Klushyn, N. Chen, R. Kurle, B. Cseke, and P. van der Smagt, “Learning hierarchical priors in VAEs,” *Advances in Neural Information processing Systems*, vol. 32, 2019.

[28] D. P. Bertsekas, *Nonlinear Programming: Second Edition*. Athena Scientific, 2003.

[29] L. Liu, H. Jiang, P. He, W. Chen, X. Liu, J. Gao, and J. Han, “On the variance of the adaptive learning rate and beyond,” *arXiv preprint arXiv:1908.03265*, 2019.

[30] H. Zhang, M. Cisse, Y. N. Dauphin, and D. Lopez-Paz, “mixup: Beyond empirical risk minimization,” *arXiv preprint arXiv:1710.09412*, 2017.

APPENDIX

A. Training

Training VAEs and CVAEs can be challenging due to local minima, posterior collapse or over-regularization [22], [23], [24]. Sequence-to-sequence models with strong decoders are often prone to posterior collapse. The authors in [25] reduced the capability of the decoder using the hierarchical decoder. Alternatively, reformulating the objective or using specialized training strategies can also alleviate some optimization problems. The authors in [26] reformulate training as a constrained optimization problem where the reconstruction term $-\mathbb{E}_{\hat{p}(x_{1:T})}\mathbb{E}_{q_\phi(z;x_{1:T})}[\log p_\theta(x_{2:T-1}|x_{1,T}, z)]$ term is constrained to achieve specific reconstruction accuracy. The authors in [27] train a hierarchical VAE model using a similar reformulation and use a scheduled pre-training of the reconstruction term. To attain a required reconstruction loss (powerful decoder) and to also avoid posterior collapse we formulate the optimization problem as

$$\begin{aligned} & \min_{\theta, \phi} 1 \\ & \text{s.t. } \mathbb{E}_{\hat{p}(x_{1:T})}\mathbb{E}_{q_\phi(z;x_{1:T})}[-\log p_\theta(x_{2:T-1}|x_{1,T}, z)] \leq \xi_{\text{rec}} \\ & \quad \mathbb{E}_{\hat{p}(x_{1:T})}\text{KL}[q_\phi(z; x_{1:T}) \| p_\theta(z; x_{1:T})] \leq \xi_{\text{kl}}. \end{aligned}$$

The resulting Lagrangian will have two multipliers λ_{rec} and λ_{kl} that adaptively re-weight the reconstruction and the KL (regularization) terms. We use the exponential method of multipliers [28], that is, we apply the update $\lambda_{\text{kl}}^{(k+1)} = \lambda_{\text{kl}}^{(k)} \cdot \exp\{\eta(-\mathbb{E}_{\hat{p}(x_{1:T})}\text{KL}[q_\phi(z; x_{1:T}) \| p_\theta(z; x_{1:T})] + \xi_{\text{kl}})\}$ and a corresponding one for λ_{rec} .

B. Architecture and computation

The computational analyses of this research used an NVIDIA GeForce GTX 1080 Ti GPU, with PyTorch version 2.1.0 for implementation.

The model’s encoder depth was set to 3, with an embedding dimension of 16, and a latent vector length of 32. The decoder was configured with 8 heads and 10 layers. For optimization, the RAdam optimizer [29], was chosen, configured with beta values of 0.9 and 0.999, and a learning rate of 0.0005. Batch sizes were 256 for the data in Cartesian space and 128 for the joint space. Mixup [30] was used as a data augmentation for the joint space data.